

Slowly balding black holes

Maxim Lyutikov

Department of Physics, Purdue University,
525 Northwestern Avenue, West Lafayette, IN 47907-2036

Jonathan C. McKinney

Department of Physics, Stanford University,
2575 Sand Hill Rd., Menlo Park, CA 94025

ABSTRACT

The “no hair” theorem, a key result in General Relativity, states that an isolated black hole is defined by only three parameters: mass, angular momentum, and electric charge; this asymptotic state is reached on a light-crossing time scale. We find that the “no hair” theorem is not formally applicable for black holes formed from collapse of a rotating neutron star. Rotating neutron stars can self-produce particles via vacuum breakdown forming a highly conducting plasma magnetosphere such that magnetic field lines are effectively “frozen-in” the star both before and during collapse. In the limit of no resistivity, this introduces a topological constraint which prohibits the magnetic field from sliding off the newly-formed event horizon. As a result, during collapse of a neutron star into a black hole, the latter conserves the number of magnetic flux tubes $N_B = e\Phi_\infty/(\pi c\hbar)$, where $\Phi_\infty \approx 2\pi^2 B_{NS} R_{NS}^3/(P_{NS}c)$ is the initial magnetic flux through the hemispheres of the progenitor and out to infinity. We test this theoretical result via three-dimensional general relativistic plasma simulations of rotating black holes that start with a neutron star dipole magnetic field with no currents initially present outside the event horizon. The black hole’s magnetosphere subsequently relaxes to the split monopole magnetic field geometry with self-generated currents outside the event horizon. The dissipation of the resulting equatorial current sheet leads to a slow loss of the anchored flux tubes, a process that balds the black hole on long resistive time scales rather than the short light-crossing time scales expected from the vacuum “no-hair” theorem.

1. Introduction

The “no hair” theorem (Misner et al. 1973) postulates that all black hole solutions of the Einstein-Maxwell equations of gravitation and electromagnetism in general relativity can be completely characterized by only three externally observable classical parameters: mass, electric charge, and angular momentum. The key point in the classical proof (*e.g.*, Price 1972) is that the outside medium is a vacuum. In contrast, the surroundings of astrophysical high energy sources like pulsars and black holes can rarely be treated as vacuum (Goldreich and Julian 1969; Blandford and

Znajek 1977; Muslimov and Tsygan 1992). The ubiquitous presence of magnetic fields combined with high (often relativistic) velocities produce inductive electric fields with electric potential drops high enough to break the vacuum via various radiative effects (curvature emission followed by a single photon pair production in magnetic field, or inverse Compton scattering followed by a two photon pair production). For example, in case of neutron stars the rotation of the magnetic field lines frozen into the crust generates an inductive electric field, which, due to the high conductivity of the neutron star interior, induces surface charges. The electric field of these induced surface charges has a component parallel to the dipolar magnetic field. These parallel electric fields accelerate charges to the energy $\mathcal{E} \sim eB_s R_s (\Omega R_0/c)^2$, where B_s and R_s are the surface magnetic field, radius of a neutron star and Ω is the angular rotation frequency. The resulting primary beam of leptons produces a dense secondary plasma via vacuum breakdown. Thus, in case of neutron stars the electric charges and currents are self-generated: no external source is needed. Rotating black holes can also lead to a similar vacuum break-down (Blandford and Znajek 1977).

In this paper we argue that the “no hair” theorem is not applicable to black holes formed from the collapse of magnetized neutron stars. In particular, we demonstrate that contrary to the prediction of the “no hair” theorem, the collapse of a rotating neutron star into the black hole results in a formation of a long lived self-generated conducting BH magnetosphere. This results from the violation of the key assumption of the “no hair” theorem, that the outside is vacuum, and allows a black hole to preserve open magnetic flux tubes that initially connect to the neutron star surface.

2. Electrodynamics of Neutron Star Collapse

2.1. Plasma Electrodynamics: the Constraint of Frozen-in Magnetic Fields

The electrodynamics of a highly conducting medium is qualitatively different from vacuum electrodynamics. The key difference is that the highly conducting plasma quickly shorts out any electric field (\vec{E}) parallel to magnetic field (\vec{B}) through the induction of electric currents (Kulsrud 2005). The condition $\vec{E} \cdot \vec{B} = 0$ introduces a constraint that the magnetic field lines are effectively frozen into plasma: each plasma element is always “attached” to a given magnetic field line.

Neutron stars possess dipolar magnetic field (Pacini 1968; Goldreich and Julian 1969) (this assumption has recently been verified by direct measurements of the structure of the pulsar magnetosphere in the double pulsar system; Lyutikov and Thompson 2005). In addition, rotation-induced poloidal (i.e. r - θ plane) currents flowing in the magnetosphere lead to opening-up to infinity of some field lines originating close to the magnetic polar line. Thus, a neutron star is surrounded by self-generated plasma and has field lines that connect its surface to infinity.

2.2. Electromagnetically Dominated Media: Force-Free Electrodynamics

Since the mass density of the self-generated plasma is many orders of magnitude smaller than the energy density of magnetic field, the plasma dynamics can be treated in the so-called force-free approximation (Gruzinov 1999), when the electromagnetic fields evolve due to forces generated by fields themselves. But the system is qualitatively different from vacuum: effectively, massless charges and currents provide the force balance $\rho_e \vec{E} + \mathbf{j} \times \vec{B} = 0$ and ensure the ideal condition $\vec{E} \cdot \vec{B} = 0$. More generally, the MHD formulation assumes (explicitly) that the second Poincare electro-magnetic invariant $\vec{E} \cdot \vec{B} = 0$ and (implicitly) that the first electro-magnetic invariant $B^2 - E^2 > 0$. This means that the electro-magnetic stress energy tensor can be diagonalized and, equivalently, that the electric field vanishes in the plasma rest frame. This assumption is important since we are interested in the limit when the matter contribution to the stress energy tensor goes to zero; the possibility of diagonalization of the electro-magnetic stress energy tensor distinguishes the force-free plasma and vacuum electro-magnetic fields (for which such diagonalization is generally not possible).

The equations of force-free electrodynamics can be derived from Maxwell equations and the constraint $\vec{E} \cdot \vec{B} = 0$. This can be done using general tensorial notation from the general relativistic MHD formulation in the limit of negligible inertia (Uchida 1997). This offers an advantage that the system of equations may be set in the form of conservation laws (Komissarov 2002). A more practically appealing formulation involves the 3+1 splitting of the equations of general relativity (Thorne et al. 1986; Zhang 1989). The Maxwell equations in the stationary Kerr metric then take the form

$$\begin{aligned}\nabla \cdot \vec{E} &= 4\pi\rho \\ \nabla \cdot \vec{B} &= 0 \\ \nabla \times (\alpha\vec{B}) &= 4\pi\alpha\vec{j} + D_t\vec{E} \\ \nabla \times (\alpha\vec{E}) &= -D_t\vec{B},\end{aligned}\tag{1}$$

where $D_t = \partial_t - \mathcal{L}_{\vec{\beta}}$ is the total time derivative, including Lie derivative along the velocity of the zero angular momentum observers (ZAMOs), ∇ is a covariant derivative and α is the delay function (in Schwarzschild geometry $\alpha = \sqrt{1 - 2M/r}$). (Relations (1) are valid if the shift function is divergence-less $\text{div } \vec{\beta} = 0$ and the metric is time-independent. For a more general formulation see Komissarov (2004, 2011).) Taking the total time derivative of the constraint $\vec{E} \cdot \vec{B} = 0$ and eliminating $D_t\vec{E}$ and $D_t\vec{B}$ using Maxwell equations, one arrives at the corresponding Ohm's law in Kerr metric (Lyutikov 2011a), generalizing the result of Gruzinov (1999):

$$\vec{j} = \frac{\left(\vec{B} \cdot \nabla \times (\alpha\vec{B}) - \vec{E} \cdot \nabla \times (\alpha\vec{E})\right) \vec{B} + \alpha(\nabla \cdot \vec{E}) \vec{E} \times \vec{B}}{4\pi\alpha B^2}.\tag{2}$$

Note that this expression does not contain the shift function $\vec{\beta}$. See also section 2.2 in McKinney (2006b) for a fully covariant derivation of the 4-current that also does not require time derivatives and is independent of the shift function.

2.3. The Black Hole Hair: the Conserved Poloidal Magnetic Flux

During neutron star collapse into a black hole, time dilation near the horizon and the frame-dragging of the horizon lead to the “horizon locking” condition: objects are dragged into corotation with the hole’s event horizon, which has a frequency associated with it of $\Omega_H \approx ac/(2r_{\text{Sc}}) = 9 \times 10^3 \text{rads}^{-1} P_{\text{NS},-3}^{-1}$, where a is the dimensionless Kerr parameter. The Kerr parameter of the resulting black hole may become fairly large,

$$a = (4\pi/5)(c/G)\chi R_{\text{NS}}^2/[P_{\text{NS}}M_{\text{NS}}] = 0.2(\chi/0.5)(R_{\text{NS}}/10\text{km})^2(1\text{msec}/P_{\text{NS}}),$$

but only for critically rotating neutron stars and stiff equations of state. In the above equation P_{NS} is the initial spin of a neutron star, χ is the central concentration parameter (Berti et al. 2005) $\chi \approx 0.5$, and we assumed a standard neutron star with mass 1.4 of the mass of the Sun. A relative smallness of the Kerr parameter a justifies that the space-time is approximately Schwarzschild.

Before the onset of the collapse, the electric currents within the neutron star create poloidal magnetic field. Rotation of the poloidal magnetic field lines and the resulting inductive electric field lead to the creation, through vacuum breakdown, of the conducting plasma and poloidal electric currents. The presence of a conducting plasma then imposes a topological constraint, that the magnetic field lines which initially were connecting the neutron star surface to the infinity must connect the black hole horizon to the infinity.

During the collapse, as the surface of a neutron star approaches the horizon, the closed magnetic field lines will be quickly absorbed by the black hole, while the open field lines (those connecting to infinity) have to remain open by the frozen-in condition. Thus, a black hole can have only open fields lines, connecting its horizon to the infinity. There is a well known solution that satisfies this condition: an exact split monopolar solution for rotating magnetosphere due to Michel (1973); it was generalized to Schwarzschild metrics by Blandford and Znajek (1977). We recently found an exact non-linear *time-dependent* split monopole-type structure of magnetospheres driven by spinning and collapsing neutron star in Schwarzschild geometry (Lyutikov 2011b). We demonstrated that the collapsing neutron star enshrouded in a self-generated conducting magnetosphere does not allow a quick release of the magnetic fields to infinity.

Thus, if a collapsing black hole can self-sustain the plasma production in its magnetosphere, the magnetic field lines that were initially connecting the neutron star surface to infinity will connect the black hole horizon to the infinity. Each hemisphere then keeps the magnetic flux that was initially connected to the infinity. For a neutron star with the surface magnetic field B_{NS} and the initial pre-collapse radius R_{NS} and period P_{NS} , the magnetic flux through each hemisphere connecting to infinity is $\Phi_{\infty} \approx 2\pi^2 B_{\text{NS}} R_{\text{NS}}^3/(P_{\text{NS}}c)$ (Goldreich and Julian 1969). Using quantization of the magnetic flux (Landau and Lifshitz 1959), this corresponds to a conserved quantum number of magnetic flux tubes

$$N_B = e\Phi_{\infty}/(\pi c\hbar) = 2\pi B_{\text{NS}} e R_{\text{NS}}^3/(c^2 \hbar P_{\text{NS}}) = 10^{41} \frac{B_{\text{NS}}}{10^{12}\text{G}} \frac{P_{\text{NS}}}{1\text{msec}}. \quad (3)$$

This quantum number is the black hole “hair”: an observer at infinity can measure the corresponding Poynting flux and infer the number N_B .

The conserved poloidal magnetic flux (3) implies a magnetic field on the horizon of the black hole

$$B_{\text{BH}} = \frac{\pi c^3 B_{\text{NS}} R_{\text{NS}}^3}{4 (GM)^2 P_{\text{NS}}} = 6 \times 10^{11} \text{G} \frac{B_{\text{NS}}}{10^{12} \text{G}} \left(\frac{P_{\text{NS}}}{1 \text{msec}} \right)^{-1}. \quad (4)$$

We can then verify that the resulting black hole will have no problem in breaking the vacuum: the rotation of the black hole leads to the appearance of the inductive electric field with a total potential drop within the magnetosphere of the order

$$\Delta\Phi \approx ae B_{\text{BH}} R_{\text{BH}} = \frac{2\pi^2}{5} \chi \frac{ec^2}{G^2} \frac{B_{\text{NS}} R_{\text{NS}}^5}{M_{\text{NS}}^2 P_{\text{NS}}^2} = 10^{19} \text{V} \frac{\chi}{0.5} \frac{B_{\text{NS}}}{10^{12} \text{G}} \left(\frac{P_{\text{NS}}}{1 \text{msec}} \right)^{-2}. \quad (5)$$

This is sufficiently high to break the vacuum via radiative effects and produce a highly conducting plasma. In addition, even in the relatively weak gravitational field of a neutron star, the general relativistic effects of the rotation of space-time (the Lense-Thirring precession) dominate the accelerating electric field (Muslimov and Tsygan 1992). The Lense-Thirring precession near the black hole also facilitates plasma production (Blandford and Znajek 1977).

3. Numerical Simulations

We have performed numerical simulations that confirm the basic principle that the “no-hair” theorem and related time-dependent vacuum simulations are not applicable to a plasma-filled black hole magnetosphere. We do not model the process of vacuum breakdown and the subsequent formation of a plasma-filled magnetosphere. Instead, we assume the neutron star already created a plasma-filled magnetosphere (or that the black hole self-generates a plasma-filled magnetosphere), and we assume that the neutron star has already collapsed to a black hole. Only once an event horizon has formed would the magnetic field begin to slip-off the black hole in vacuum, so starting with an event horizon should be a strong enough test – one should not have to follow the collapse of the neutron star to a black hole as long as a plasma is present. The goal of the simulations is to measure the decay timescale of the magnetic flux threading the event horizon of the black hole: $\Phi_{\text{EM}} = (1/2) \int_S dS |B^r|$ as integrated over the surface (S) of the black hole horizon. We show that the magnetic dipole decay seen in vacuum solutions is avoided or delayed by three effects: 1) presence of plasma and self-generation of toroidal currents ; 2) black hole spin induced poloidal currents ; and 3) plasma pressure support of current layers generated internally by dissipating currents. These effects cause the field to avoid vacuum-like decay of the dipole magnetic field and help support the newly-formed split-monopole magnetic field against magnetic reconnection.

These GRMHD simulations use the fully conservative, shock-capturing GRMHD scheme called HARM (Gammie et al. 2003; McKinney & Gammie 2004; McKinney 2006a,b; Noble et al. 2006) using Kerr-Schild coordinates in the Kerr metric for a sequence of spins given by $\{a = 0, 0.1, 0.5, 0.9, 0.99\}$

(in such models without a disk, negative spin is not physically distinct from positive spin). The code includes a number of improvements (Mignone & McKinney 2007; Tchekhovskoy et al. 2007, 2008, 2009) compared to the original code. This code is capable of choosing the equations of motion as MHD, force-free electrodynamics, and vacuum electrodynamics. The code permits full 3D (no assumed symmetries) simulations as reported in McKinney & Blandford (2009).

We perform simulations that either use the force-free or use the fully energy-conserving MHD equations of motions. These approximate, respectively, the limits of radiatively efficient emission and radiatively inefficient emission once the plasma has been generated. That is, if the electromagnetic field dominates the rest-mass and internal energy density over most of the volume outside current sheets, then the force-free limit corresponds to an instantaneous loss (such as radiation) of magnetic energy dissipated in current sheets, while the fully energy-conserving MHD limit without cooling corresponds to all dissipated energy going into internal+kinetic energy that remains in the system and sustains the current sheet against dissipation. A non-energy-conserving system of equations or simulation code would be unable to properly follow the energy conservation process of electromagnetic dissipation within the current sheet that leads to plasma formation there. The force-free electrodynamics equations of motion are not solely relied upon because they are undefined within current sheets and any particular resistive force-free electrodynamics equations (Lyutikov 2003; Gruzinov 2008; Li et al. 2011) still leave some degree of ambiguity in how the resistivity would map onto the full magnetohydrodynamical (MHD) equations. For the MHD equations, an ideal $\gamma = 4/3$ gas equation of state is chosen, which can be considered as mimicking a radiatively inefficient high-energy particle distribution component generated by the dissipation of the currents within the reconnecting layer.

The initial condition corresponds to a NS dipole field given by an orthonormal ϕ -component of the vector potential of $A_\phi \propto \sin\theta/r^2$ with no rotation and no ϕ component of the magnetic field present at the initial time. This initial magnetic field corresponds to the exterior dipole solution for a neutron star, but the metric has simply been chosen as a Kerr metric in Kerr-Schild form. This forces the black hole alone to produce any and all currents exterior to the horizon, and so the simulations represent an even more general test of the horizon locking condition described in the prior sections.

For MHD models, the magnetosphere is filled with only a low-density atmosphere of rest-mass density and internal energy density, such that the electromagnetic energy density exceeds both by factors of ten or more through-out the simulation. During the MHD simulations, near the black hole at the stagnation surface (zero radial velocity, where plasma must be created) mass-energy is injected in a zero angular momentum observer (ZAMO) frame to maintain a high magnetization of roughly $\mu \sim 100$ times more electromagnetic energy than rest-mass energy. As long as $\mu \gg 1$, the details of how this injection is done do not affect the results (Tchekhovskoy et al. 2010). For force-free simulations, the condition $B^2 - E^2 > 0$ is enforced as an immediate loss (e.g. by radiation) of energy-momentum as described in McKinney (2006b). The initial velocity field is set to be that of a ZAMO (McKinney & Gammie 2004). We have now completely specified the metric, initial value

problem, and equations of motion used.

These models are simulated with increasing resolution to seek convergence or the trend on results with resolution. The models have radial resolutions of $N_r = \{64, 128, 256\}$ cells, θ resolutions of $N_\theta = \{32, 64, 128\}$ cells, and ϕ resolutions of $N_\phi = \{1, 16, 32\}$ cells in order to seek the lowest-order ϕ dependence. The simulation grid resolution is focused on the magnetosphere near the black hole, while also extending to large radii to avoid artificial interactions with the outer radial boundary. The radial grid from 0.9 times the event horizon radius (r_H) to $10^4 GM/c^2$ is defined by the exponential $r = 0.5 + \exp(x_1)$ with $x_1 \propto i/N_r$ for grid element i up to a break radius of $r = 100 GM/c^2$ for an easily computable $x_{1,\text{br}}$, after which the grid becomes hyper-exponential such that value of x_1 adds to itself $(x_1 - x_{1,\text{br}})^2$ for each $i > i_{\text{br}}$. The grid in θ goes from 0 to π and is uniform. The grid in ϕ goes from 0 to 2π and is also uniform. The simulations are run for a time $1000 GM/c^3$ in order to reach a quasi-steady state.

At the low resolutions considered for these simulations, dissipation is enhanced compared to expected at high resolutions. So the simulations only place lower limits on a measurement of the decay timescale of the magnetic flux threading the black hole event horizon. A convergent solution implies the result is independent of any microscopic resistivity model and only depends upon the self-consistently generated turbulent resistivity. A non-convergent result would imply the microscopic resistivity controls the dissipation and must be specified. For such a non-convergent case, we can estimate the expected resistivity (Uzdensky & McKinney 2011), such as done in the next section.

Figure 1 shows the initial and quasi-steady contour plots for $\Psi = RA_\phi$ for the axisymmetric $256 \times 128 \times 1$ resolution and black hole with spin $a = 0.99$. The initial dipole field has collapsed to essentially a split monopole field with most of the magnetic flux passing through the horizon instead of reconnecting near the equator. This was predicted by Lyutikov (2011b). All other models at different spins show qualitatively similar final states, except the 3D simulations with resolution $256 \times 128 \times 16$ or $256 \times 128 \times 32$ show slightly more closed field structures at the equator beyond the event horizon.

Figure 2 shows the value of magnetic flux Φ_{EM} vs. time (t) for all black hole spins and both the force-free electrodynamics equations of motion (radiatively efficient regime) and the MHD equations of motion (radiatively inefficient regime). At $t = 0$, the black hole rotation begins to drive radial currents into the magnetosphere. Then, during the first $t \sim 20 GM/c^3$, some portion of the dipole field is absorbed by the black hole. For high black hole spin rates, the amount of lost magnetic flux is found to correspond to losing those field lines that do not cross the Alfvén surface ($R \sim \Omega_F/c \approx \Omega_H/(2c)$, for field rotation frequency Ω_F) at late times. This means that those field lines that eventually open-up to infinity are prevented from being absorbed by the black hole by the poloidal currents driven into the magnetosphere by the rotation of the black hole. For low black hole spin rates, such as for $a = 0$, the early loss of magnetic flux is limited by the equatorial toroidal current sheet that forms over a timescale of $t \sim 25 GM/c^3$, which corresponds to the light-crossing

timescale over a wavelength of $\lambda \approx 24.7GM/c^2$ for electromagnetic radiation from the decay of a dipole field for a vacuum Schwarzschild black hole (Baumgarte & Shapiro 2003). This means that the decay by vacuum radiation is avoided by toroidal current sheet formation due to collapse of the dipole field in the presence of a plasma. Overall, decay of the dipole field is avoided by poloidal and toroidal currents that spontaneously form due to black hole rotation and collapse of the dipole field in the presence of a plasma.

For the MHD solutions, over the first $t \sim 50GM/c^3$, the solution then settles into a quasi-steady state of a roughly constant magnetic dissipation near the black hole. The dissipation creates plasma pressure within the current layer that supports the layer against magnetic reconnection. The decays are fit well by an exponential decay, where the decay timescale for the 256×128 resolution for the MHD models with $a = \{0, 0.1, 0.5, 0.9, 0.99\}$ is $\tau \sim \{100, 110, 120, 400, 500\}GM/c^3$, respectively. As expected for the discontinuity resolved at the numerical grid scale, the decay timescale is found to be directly proportional to the resolution (i.e. $\tau \propto \{N_r, N_\theta, N_\phi\}$). Otherwise identical 3D models show larger decay timescales, so even higher resolution 3D models (i.e. $N_\phi > 32$) should not be required to find a lower limit on the decay timescale.

This figure also shows that the radiative efficiency of the current layer is crucial to whether the magnetosphere survives for long periods of time. The force-free solutions continue rapid dissipation due to a lack of plasma pressure within the current layer. The decay timescale at this resolution for the force-free models is $\tau \sim 10GM/c^3$ for $a = 0$ and $\tau \sim 20GM/c^3$ for $a = 0.99$. The force-free simulations show a decay timescale comparable to vacuum dipole decay on a black hole, which decays as $\sim (t - 19)^{-4}$ starting after only $t \sim 20GM/c^3$ (Baumgarte & Shapiro 2003). A force-free simulation code with less dissipation may help avoid such fast dissipation in the force-free limit (e.g. Spitkovsky 2006), unless the condition $B^2 < E^2$ is still manifested within the current layer because then a causal force-free solution requires dissipation in order to recover the causal condition $B^2 > E^2$.

This figure also shows that non-zero black hole spin induction of poloidal currents cause an extension of the timescale for dissipation of the magnetosphere in either the force-free or MHD limits.

Overall, the field lines that were initially connected to the surface of the neutron star (that would have reached to infinity for a rotating magnetosphere) remain connected to the black hole horizon for times much longer than $\sim 20GM/c^3$ that is predicted by the “no-hair” theorem. In case of an initial magnetic field corresponding to the aligned pulsar, those field lines that are associated with the closed part of the magnetosphere are absorbed by the black hole, while those field lines that would reach to infinity for the neutron star magnetosphere are forced to become open by poloidal currents driven into the magnetosphere by the black hole rotation.

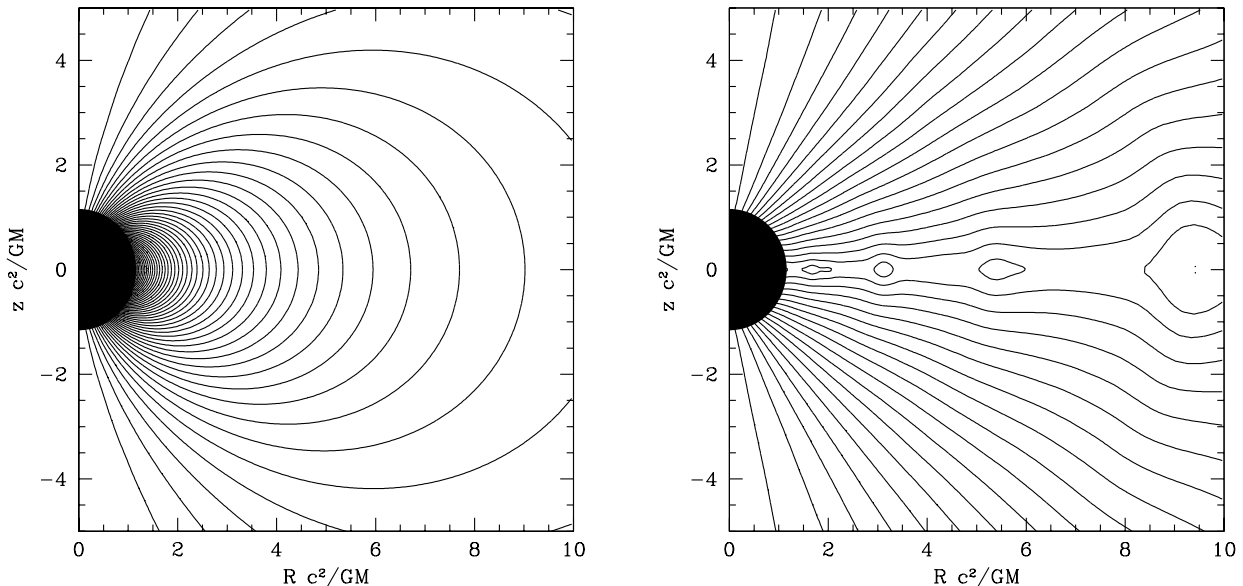


Fig. 1.— A contour plot of the magnetic flux ($\Psi = RA_\phi$) showing the inner (cylindrical radius) $R < 10GM/c^2$ for the MHD $a = 0.99$ model described in the text. The initial magnetic field configuration corresponds to a neutron star type dipolar field where there are no currents outside the event horizon. The left panel shows the initial time, while the right panel shows the solution at $t = 1000GM/c^3$. The structure of the magnetosphere relaxes to monopolar-like solution, as predicted by Lyutikov (2011b). Note also the development of the tearing modes and the formation of magnetic islands in the equatorial current sheet.

4. Slowly balding black hole

As we showed above through analytical estimates and numerical simulations, the magnetosphere of a newly formed black hole relaxes to a split-monopole-type structure. The resulting current sheet is subject to resistive dissipation that would reconnect the field lines from the different hemispheres, producing a set of closed field lines that will be quickly absorbed by the black hole and a set of open field lines that will be released to infinity in an event qualitatively similar to solar coronal mass ejections (CMEs) (Aschwanden 2005). This will lead to a decrease of the number of magnetic flux tubes through each hemisphere N_B . The black hole will be slowly balding. This “hair loss” will proceed on the resistive time scale of the equatorial current sheet. Typically, resistive time scales in a plasma are much longer than the dynamical times scales by a factor of the so-called Lundquist (magnetic Reynolds) number.

Reconnection of magnetic field lines is a notoriously difficult problem in plasma physics (Kulsrud 2005). Development of plasma turbulence in the regions of strong current and the resulting

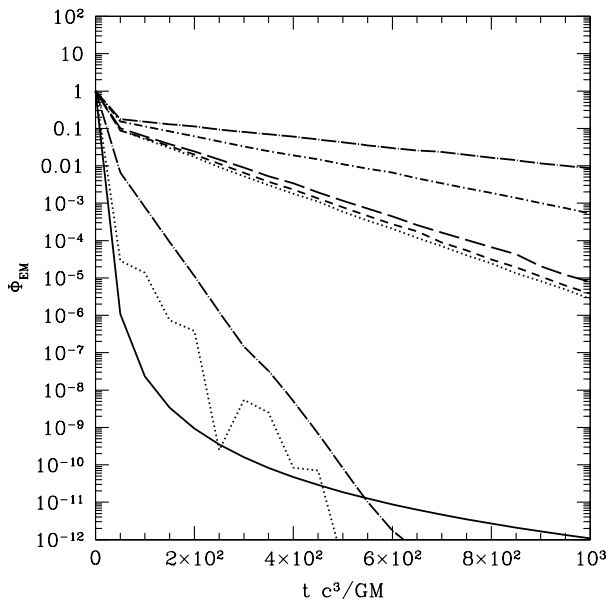


Fig. 2.— The value of magnetic flux Φ_{EM} divided by its initial ($t = 0$) value vs. time (t) for the different black hole spins and equations of motion (force-free and MHD). The MHD models for spins $\{a = 0, 0.1, 0.5, 0.9, 0.99\}$ correspond to $\{\text{dot}, \text{shortdash}, \text{longdash}, \text{dot} - \text{shortdash}, \text{dot} - \text{longdash}\}$ line types appearing in the upper part of the plot. The force-free models for spins $\{a = 0, 0.99\}$ correspond to $\{\text{dot}, \text{dot} - \text{longdash}\}$ line types and appear at the lower part of the plot. The analytical $(t - 19)^{-4}$ decay for a vacuum dipole on a black hole is shown as a solid line and appears in the lower part of the plot. Notice that for the radiatively inefficient MHD regime, magnetic flux “slides off” the black hole on time scales much longer than those predicted by the “no hair” theorem that follows t^{-4} . Also note that the $a = 0$ model only mimics a slowly rotating NS that still allows a plasma magnetosphere to be self-generated.

anomalous resistivity, plasma collisionality (McKinney & Uzdensky 2010), as well as formation of localized narrow current sheets may bring significant variations in the dissipation time scale.

As a possible estimate of the reconnection time scale, let us assume that the reconnection is driven by charge starvation as applicable to our model. A charge-neutral plasma of a given density n can support a current no larger than $j \leq 2nec$. Thus, for a given magnetic field B and density n there is a minimum thickness of a current layer $\delta \approx B/(2\pi en)$.

The black hole magnetosphere extends from the horizon R_{BH} to the light cylinder located at $R_{\text{LC}} = c/\Omega_H$. General relativistic effects of time dilation would effectively freeze out the reconnection process near the horizon. Let us next estimate the reconnection rate near the light cylinder of the resulting black hole. Taking δ as a thickness of the resistive layer of total length $L \sim R_{\text{LC}}$, we can estimate the Lundquist (magnetic Reynolds) number within, *e.g.*, the Sweet-Parker (Kulsrud

2005) model of reconnection, $S = (R_{LC}/\delta)^2$. In a highly magnetized plasma the Sweet-Parker reconnection inflow velocity is $v_{\text{in}} \sim c/\sqrt{S}$.

The expected density can be scaled to the local Goldreich-Julian density (Goldreich and Julian 1969), $n = \lambda n_{GJ}$. Taking the angular velocity of field lines equal to Ω_H , then $n_{GJ} = B\Omega_H/(2\pi ec)$. The multiplicity λ is expected to be high, $\lambda \gg 1$ (Ruderman and Sutherland 1975). We then find the Lundquist number $S = 16\lambda^2$ and reconnection time scale $\tau_{\text{rec}} = 4\lambda R_{LC}/c$, which can be written as

$$\frac{\tau_{\text{rec}}}{R_{\text{BH}}/c} \approx \frac{\lambda}{\chi} \frac{R_{\text{BH}} c P_{\text{NS}}}{R_{\text{NS}}^2} = 10^5 \left(\frac{\chi}{0.5} \right)^{-1} \frac{\lambda}{10^5} \frac{P_{\text{NS}}}{1\text{msec}}. \quad (6)$$

This is much longer than the light travel time over the horizon of the black hole.

The above estimate of the reconnection rate is given mostly for illustrative purposes. Various reconnection-type phenomena may produce vastly different time scales. For example, the development of a tearing mode in the relativistic magnetized plasma proceeds on the tearing mode time scale, which is intermediate between the dynamic and the resistive time scales (Lyutikov 2003; Komissarov et al. 2007). In general, the dissipation timescale is much longer than the dynamical time scale due to the formation of self-generated currents outside the event horizon and due to the formation of plasma pressure within the current sheet.

5. Discussion

We found that the “no hair” theorem is not applicable to a rotating neutron star collapsing into a black hole. As long as the black hole is able to self-produce a highly conducting plasma via the vacuum breakdown, the magnetic field cannot “slide off” the black hole. The presence of a highly conducting plasma introduces a topological constraint for magnetic fields lines. If the magnetospheric plasma were ideal, the “no hair” theorem would be truly inapplicable. Only the introduction of a finite resistivity, that leads to a violation of the frozen-in condition, results in loss of the magnetic field lines. As a result, a black hole retains magnetic field for long resistive time scale and not the dynamical time scale $\sim GM/c^3$ predicted by the “no hair” theorem. Thus, a black hole can produce an electromagnetic power for a long time after the collapse, without a need for an externally supplied magnetic field.

The principal difference from the conventional Blandford-Znajek Blandford and Znajek (1977) picture of AGN jet launching is that in that case the magnetic field is brought from outside, electric currents are supported by externally supplied accretion material. In our case there is no outside-provided plasma: the currents all are self-generated. The initial poloidal magnetic field of a NS is necessary to create the black hole magnetosphere. The neutron star’s rotation can create poloidal currents outside what will become the event horizon. After the collapse, the initial toroidal currents of the dipole field are consumed by the BH. Our simulations show that, even without existing external poloidal or toroidal currents, the rotation of the newly formed black hole

alone can create new monopolar currents outside the horizon that can survive for times much longer than the collapse time.

The fact that a black hole resulting from a collapse of magnetized rotating progenitor retains the progenitor’s magnetic field may have important astrophysical implications, especially in gamma ray burst (GRB) research, allowing electromagnetic extraction of energy from isolated black holes. The black hole resulting from a collapse of a neutron star will rotate with angular velocity

$$\Omega_H \approx \frac{\chi}{5} \frac{c^4 R^2 \Omega}{G^2 M_{NS}^2}. \quad (7)$$

The collapse of the rotating neutron star into the black hole preserves the open magnetic flux

$$\Phi_0 = \pi R_{NS}^2 B_{NS} \left(\frac{R_{NS} \Omega}{c} \right). \quad (8)$$

The flux Φ_0 will produce magnetic field on the black hole $B_{BH} \approx \Phi_0 / (2\pi R_{BH}^2)$. The spin-down of the resulting magnetized black hole will produce an electromagnetic wind with luminosity (Michel 1973; Komissarov 2001; McKinney & Gammie 2004; McKinney 2005; Tchekhovskoy et al. 2010, 2011)

$$L_{BH} \approx \frac{2}{3c} \left(\frac{\Omega_H \Phi_0}{4\pi} \right)^2 = \frac{2\pi^4}{75} \chi^2 \frac{c^5}{G^4} \frac{B_{NS}^2 R_{NS}^{10}}{M_{NS}^4 P_{NS}^4} \approx 10^{43} \text{ ergs}^{-1} \left(\frac{\chi}{0.5} \right)^2 \left(\frac{B_{NS}}{10^{12} \text{ G}} \right)^2 \left(\frac{P_{NS}}{1 \text{ msec}} \right)^{-4}. \quad (9)$$

This black hole power drives a jet that can reach high Lorentz factors at large radii (McKinney 2006a; Barkov & Komissarov 2008). For the chosen value of the neutron star magnetic field, this is a fairly low power, but it can become observable if magnetic field is amplified during the collapse to magnetar values of $\sim 10^{14}$ – 10^{15} Gauss (Thompson and Duncan 1993). If this indeed happens, the rotational power of the black hole extracted by magnetic fields may power the prompt GRB emission (Usov 1992) or early afterglows (Lyutikov 2010).

We would like to thank Scott Hughes, Serguei Komissarov and Luis Lehner for many insightful comments and the National Institute for Nuclear Theory for hospitality.

REFERENCES

- M. J. Aschwanden, *Physics of the Solar Corona. An Introduction with Problems and Solutions (2nd edition)* (2005).
- Baumgarte, T. W., & Shapiro, S. L. 2003, ApJ, 585, 930
- E. Berti, F. White, A. Maniopoulou, and M. Bruni, MNRAS **358**, 923 (2005), [arXiv:gr-qc/0405146](#).
- R. D. Blandford and R. L. Znajek, MNRAS **179**, 433 (1977).

- Gammie, C. F., McKinney, J. C., & Tóth, G. 2003, ApJ, 589, 444
- P. Goldreich and W. H. Julian, ApJ **157**, 869 (1969).
- A. Gruzinov, ArXiv Astrophysics e-prints (1999), [astro-ph/9902288](#).
- A. Gruzinov, ArXiv e-prints (2008), [0802.1716](#).
- Komissarov, S. S. 2001, MNRAS, 326, L41
- S. S. Komissarov, MNRAS **336**, 759 (2002), [arXiv:astro-ph/0202447](#).
- S. S. Komissarov, MNRAS **350**, 427 (2004), [arXiv:astro-ph/0402403](#).
- S. S. Komissarov, M. Barkov, and M. Lyutikov, MNRAS **374**, 415 (2007), [arXiv:astro-ph/0606375](#).
- Barkov, M. V., & Komissarov, S. S. 2008, MNRAS, 385, L28
- S. S. Komissarov, ArXiv e-prints (2011), [1108.3511](#).
- R. M. Kulsrud, *Plasma physics for astrophysics* (2005).
- L. D. Landau and E. M. Lifshitz, *Statistical Mechanics* (1959).
- J. Li, A. Spitkovsky, and A. Tchekhovskoy, ArXiv e-prints (2011), [1107.0979](#).
- M. Lyutikov, MNRAS **346**, 540 (2003), [arXiv:astro-ph/0303384](#).
- M. Lyutikov and C. Thompson, ApJ **634**, 1223 (2005), [arXiv:astro-ph/0502333](#).
- M. Lyutikov, in *The shocking Universe*, edited by G. Chincarini, P. D’Avanzo, R. Margutti, and R. Salvaterra (2010), pp. 3–33, [arXiv:astro-ph/0911.0349](#).
- M. Lyutikov, Phys. Rev. D **83**, 064001 (2011a), [1101.0639](#).
- M. Lyutikov, ArXiv e-prints (2011b), [1104.1091](#).
- McKinney, J. C., & Gammie, C. F. 2004, ApJ, 611, 977
- J. C. McKinney, ApJ **630**, L5 (2005), [arXiv:astro-ph/0506367](#).
- McKinney, J. C. 2006, MNRAS, 367, 1797
- McKinney, J. C. 2006, MNRAS, 368, 1561
- McKinney, J. C., & Blandford, R. D. 2009, MNRAS, 394, L126
- McKinney, J. C., & Uzdensky, D. A. 2010, [arXiv:1011.1904](#)

- F. C. Michel, ApJ **180**, 207 (1973).
- C. W. Misner, K. S. Thorne, and J. A. Wheeler, *Gravitation* (San Francisco: W.H. Freeman and Co., 1973, 1973).
- A. G. Muslimov and A. I. Tsygan, MNRAS **255**, 61 (1992).
- Noble, S. C., Gammie, C. F., McKinney, J. C., & Del Zanna, L. 2006, ApJ, 641, 626
- F. Pacini, Nature **219**, 145 (1968).
- R. H. Price, Phys. Rev. D **5**, 2439 (1972).
- M. A. Ruderman and P. G. Sutherland, ApJ **196**, 51 (1975).
- Tchekhovskoy, A., McKinney, J. C., & Narayan, R. 2007, MNRAS, 379, 469
- Mignone, A., & McKinney, J. C. 2007, MNRAS, 378, 1118
- Tchekhovskoy, A., McKinney, J. C., & Narayan, R. 2008, MNRAS, 388, 551
- Tchekhovskoy, A., McKinney, J. C., & Narayan, R. 2009, ApJ, 699, 1789
- Tchekhovskoy, A., Narayan, R., & McKinney, J. C. 2010, ApJ, 711, 50
- Tchekhovskoy, A., Narayan, R., & McKinney, J. C. 2011, arXiv:1108.0412
- K. S. Thorne, R. H. Price, and D. A. MacDonald, *Black holes: The membrane paradigm* (Black Holes: The Membrane Paradigm, 1986).
- Spitkovsky, A. 2006, ApJ, 648, L51
- C. Thompson and R. C. Duncan, ApJ **408**, 194 (1993).
- Uzdensky, D. A., & McKinney, J. C. 2011, Physics of Plasmas, 18, 042105
- T. Uchida, Phys. Rev. E **56**, 2181 (1997).
- V. V. Usov, Nature **357**, 472 (1992).
- X. Zhang, Phys. Rev. D **39**, 2933 (1989).